Barker, P. F., Kennett, J. P., et al., 1990
Proceedings of the Ocean Drilling Program, Scientific Results, Vol. 113

19. SEDIMENTARY RESPONSE TO PALEOCLIMATE FROM DOWNHOLE LOGS AT SITE 693, ANTARCTIC CONTINENTAL MARGIN[1]

Xenia Golovchenko,[2] Suzanne B. O'Connell,[3] and Richard Jarrard[2]

ABSTRACT

The first well logs collected below the Antarctic circle were obtained during Leg 113 at Site 693 on the Dronning Maud Land Margin (Antarctica) in the Weddell Sea. Gamma-ray, resistivity, and sonic logs were collected between 108.0 and 439.0 mbsf. The downhole logs show good agreement with the data collected from cores and provide a continuous measurement of the sedimentary record. These continuous log records show that the rather uniform Tertiary lithology seen in cores is characterized by high-frequency variability in the log data. Several thin hard streaks are identified, the largest of which coincides with a major Miocene hiatus. Associated with this hiatus is a change to lower illite content (and correspondingly lower gamma-ray counts) and to a significant increase in diatom content.

Spectral analysis of the logs was performed on the lower Pliocene through upper Oligocene interval (108.0–343.0 mbsf). Between 108.0 and 245.0 mbsf, average sedimentation rates (50 and 26 m/m.y.) are high enough to show that variance is present in the orbital eccentricity (~95 k.y.) and obliquity (~41 k.y.) bands. Between 253.0 and 343.0 mbsf, the sedimentation rate (8 m/m.y.) is too low to resolve high frequency variations. The Milankovitch frequencies are best developed in the resistivity logs. Resistivity is responding to changes in porosity, which in these sediments is controlled by the abundance of biosiliceous sediments, particularly diatoms. The orbital forcing suggested by the Milankovitch frequencies may be influencing diatom productivity by inducing oscillations in upwelling, ice coverage, pack ice, and/or polynya. Although variations in diatom abundance were observed in the cores, they were not attributed to a Milankovitch signal, and therefore in this environment, downhole logs are an important contribution to the detection and understanding of orbitally influenced changes in sedimentation.

INTRODUCTION

ODP Site 693 lies in 2359 m of water on a mid-slope bench on the main northwest-facing slope of the Dronning Maud Land margin (Antarctica) in the Weddell Sea (Fig. 1). Two holes were drilled to obtain information about the evolution of the Antarctic continental climate through the Cenozoic. Hole 693A was rotary cored to 483.9 mbsf. Hole 693B was cored with the extended core barrel (XCB) from 233.8 to 262.7 mbsf and from 287.2 to 402.9 mbsf; between 262.8 and 287.1 mbsf, the hole was cored with the advanced hydraulic piston corer (APC). Recovery ranged from 0% to 100% (Fig. 2).

In Hole 693A, one logging run was made between 108.0 and 439.0 mbsf with the seismic stratigraphic tool string, which measures traveltime (borehole compensated sonic tool), relative abundance of sand and coarse silt and clay (gamma ray), resistivity (dual induction), and hole conditions (caliper). Traveltimes are expressed by two curves: DT (2.4–3.0 m spacing), and the DTL (3.0–3.7 m spacing), which has the deeper investigation of the two. Velocity, calculated by taking the reciprocal of interval traveltime, is dependent upon both lithology and porosity. Resistivity logs express the resistivity of the formation at two different depths of penetration and respond primarily to porosity variations. The gamma-ray curve provides a qualitative evaluation of clay or shale content because radioactive elements tend to concentrate in shales and clay.

In this study, log patterns in the interval between 108.0 and 397.8 mbsf (lower Pliocene to middle lower Oligocene) are interpreted from the standpoints of sedimentological variations, and of cyclic changes which may correspond to Milankovitch frequencies attributed to orbital forcing. Below 397.8 mbsf, in the lower Cretaceous sediments, the age control is too poor to establish any sedimentation rates and therefore determine cyclic changes.

The log data are compared and contrasted with core data, to obtain a synthesis of both. Log data are recorded every 15 cm, giving a sample spacing of 6.56 samples/m. Average core recovery for this interval was 40%. Exact (<5 m) depth correlation between the logs and cores is not feasible because of possible logging cable stretch, and because it is difficult to determine where within the cored interval the recovered sediment lies.

LITHOSTRATIGRAPHIC OVERVIEW

The logged interval discussed in this paper (108.0–397.8 mbsf) encompasses three lithologic units and three subunits (Fig. 2; Shipboard Scientific Party, 1988b). Lithologic Unit III (31.4–325.8 mbsf) consists dominantly of clay and silt, with diatom abundance ranging from 10% to 65%. It has been divided into three subunits on the basis of variations in nannofossil and diatom abundance observed on smear slides.

Subunit IIIA, 31.4–243.9 mbsf, consists of diatom mud and diatom clay with minor occurrences of diatom ooze and silicoflagellate-bearing diatom mud (classification scheme is described in Shipboard Scientific Party, 1988a). The clay minerals are dominated by illite and smectite, until about 165.0 mbsf. Between 165.0 and 260.0 mbsf, illite is dominant with chlorite and kaolinite and very minor smectite (Robert and Maillot, this volume). Within the terrigenous component there is a minor increase in silt-size particles downcore. Core recovery within this interval was poor (Fig. 2).

The observed sand component consists of unsorted grains from the top of the hole until 150.0 mbsf. Between approximately 150.0 and 243.9 mbsf there is a gradual transition to sediments that contain a well-sorted, very fine sand mode with a coarse tail. Dropstones of millimeter size and larger occur irregularly throughout the unit. The unit ranges in age from early Pliocene to late Miocene, with no detected hiatuses.

[1] Barker, P. F., Kennett, J. P., et al., 1990. *Proc. ODP, Sci. Results*, 113: College Station, TX (Ocean Drilling Program).
[2] Borehole Research Group, Lamont-Doherty Geological Observatory, Palisades, NY 10964.
[3] Department of Earth and Environmental Sciences, Wesleyan University, Middleton, CT 06547.

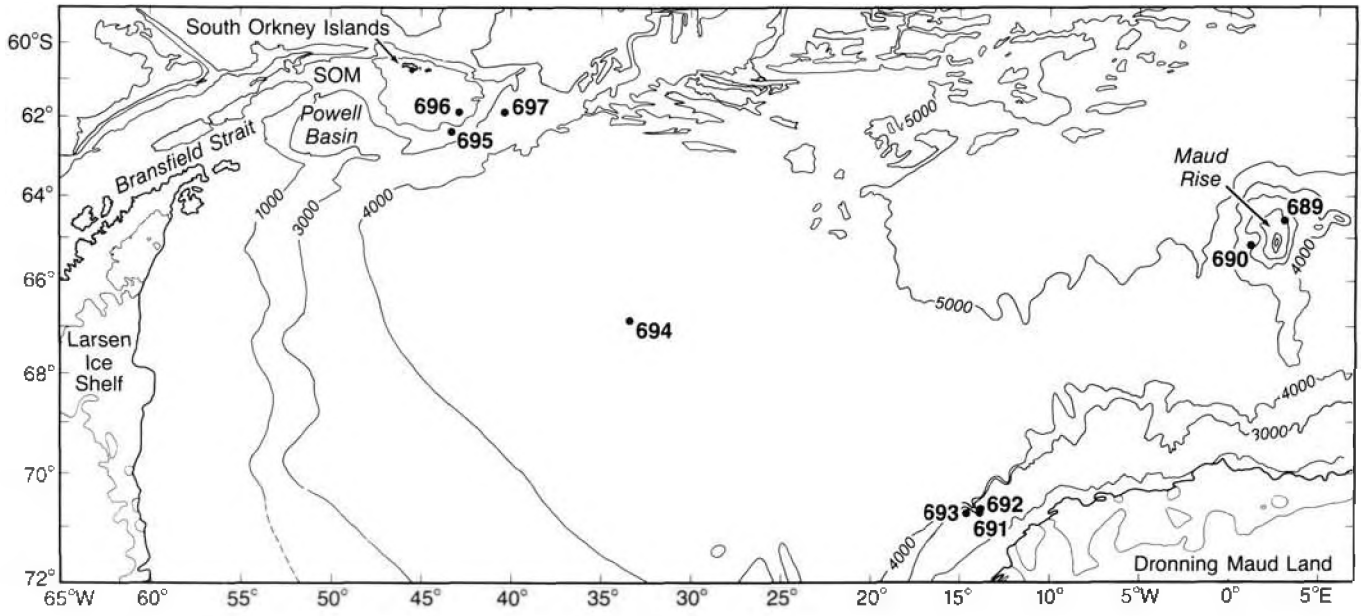

Figure 1. Site location map for Site 693 (from Shipboard Scientific Party, 1988b). Contours are in uncorrected meters.

Subunit IIIB, 243.9–255.1 mbsf, is distinct in an otherwise relatively homogeneous unit because of the presence of nannofossils, accompanied by a decrease in the terrigenous component.

Subunit IIIC, 255.1–325.8 mbsf, was cored with both the extended and rotary core barrels. Despite this, both core quality and recovery were generally poor. The sediments are similar to those of Subunit IIIA; i.e., diatom mud, clay, and ooze. Illite is the dominant clay mineral. The percentage of sand remains constant, but the clay content increases gradually downhole at the expense of the silt component. Sand layers, with sharp basal contacts and diffuse tops, were recovered between 268.4 and 276.0 mbsf and at 279.0 mbsf. Dropstones are common. The unit ranges in age from early Miocene to late Oligocene. The lower Miocene section contains a hiatus at 262 mbsf which spans about 7 m.y. over the lower upper and middle Miocene.

Lithologic Unit IV, 325.8–345.1 mbsf, contains both calcareous and siliceous biogenic, centimeter-thick cycles, interbedded with dominantly terrigenous sediments. The cycles can be identified on the basis of color since the diatom-rich sediments are darker than the nannofossil-rich sediments. The most developed carbonate layer is present in Core 113-693A-36R, 0–10 cm (331 mbsf), where smear slide data indicate 85% nannofossils. The terrigenous component (both clay and sand) increases downhole. Dropstones, millimeters across, are present but rare. Both core recovery and quality are generally moderate.

Lithologic Unit V, 345.1–397.8 mbsf, consists of diatomaceous mud and silt that has been thickened and deformed by slumping. The entire interval is within a single, very short diatom zone. Reworked Tertiary, Mesozoic, and Paleozoic pollen are found in the lowermost few meters of the unit (Shipboard Scientific Party, 1988b). Near the base of the unit at 388.0–393.0 mbsf is a bed identifiable on the logs as very high in porosity and slightly reduced in clay content. This bed is likely to be a clayey diatomite; because of its low strength it may well have been the layer on which slump failure occurred.

Capping the inferred diatomite is a 19 m interval that is remarkably similar in gamma-ray character to the 19 m interval that overlies it (Fig. 3). Possibly the interval 368.0–351.0 mbsf is a repeat section that has slumped onto the 387.0–368.0 mbsf section. If so, the lower interval could be largely in place; however, it did not escape some slump-related disturbance, because disturbed bedding is evident in cores throughout the unit. The speculative repeat section is not readily testable from the limited core recovery.

LOG ANALYSIS

Porosity and Velocity

The medium-induction resistivity log from Site 693 has been converted to a log of apparent porosity (Shipboard Scientific Party, 1988b), based on the method of Doveton (1986). The conversion assumes that the sediments contain no clay minerals, an assumption that is certainly invalid at Site 693. However, the sediments recovered at this site exhibit porosities well over 50% (Fig. 4); therefore, this assumption leads to only a slight overestimation of porosity (Jarrard et al., in press).

Compaction is expected to cause a decrease in porosity and increase in velocity with depth at Site 693. These changes are evident in both laboratory and log measurements of porosity (Fig. 4) and velocity (Fig. 5). However, as discussed below, only the log measurements of velocity are considered to reflect accurately the compaction at Site 693.

Figure 4 compares porosities calculated from the resistivity log to those determined by laboratory measurements on discrete samples. The laboratory porosity measurements on rotary samples from between 110.0 and 150.0 mbsf are 8–25 porosity units higher than porosities determined from the resistivity log. The poor correlation is attributed to the almost complete remolding of the rotary cored sediments. Below 150.0 mbsf the correlation improves but is still variable. Below 180 mbsf, sediments are sufficiently compacted to resist the disturbing effects of rotary coring, and core porosity shows a systematic compaction-related decrease with depth. The correlation between data sets is very good in the less disturbed XCB cores (234.0–403.1 mbsf, Fig. 4).

Even in the "undisturbed" cores below 180.0 mbsf, core measurements are likely to overestimate porosity by 2–4 porosity units because of rebound, the expansion that the core undergoes when removed from *in situ* pressures (Hamilton, 1976). This ef-

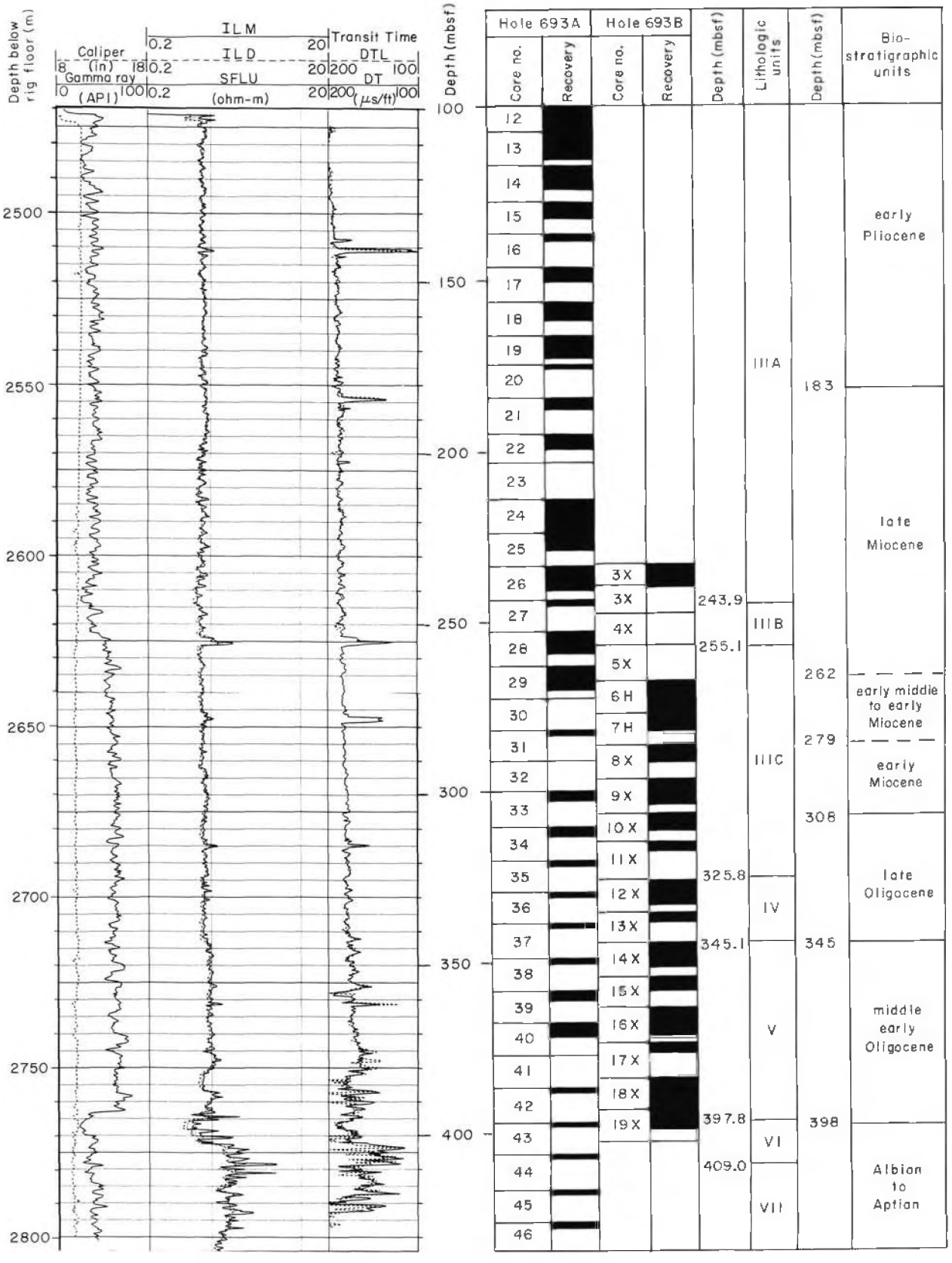

Figure 2. Core recovery, lithostratigraphic units, age, and well logs for Site 693, 100.0–435.0 mbsf. Hole 6893A was cored with the rotary corer (RCB), and Hole 693B was cored with both the advanced hydraulic piston corer (APC) and the extended core barrel (XCB).

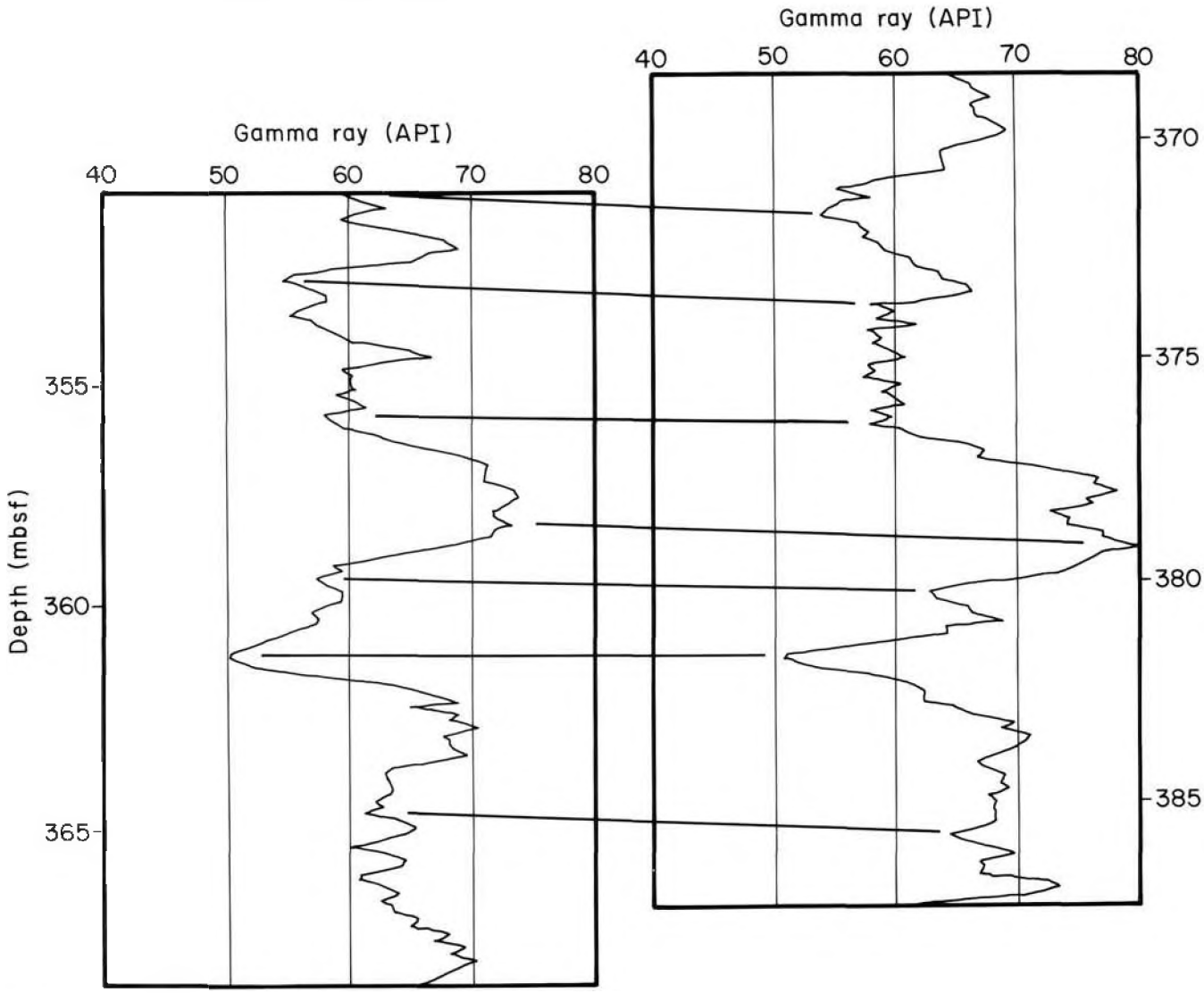

Figure 3. Comparison of gamma-ray changes over two portions of an interval with slump structures, showing a possible repeat section.

fect is too subtle to degrade the correlation observed in Figure 4 between laboratory and log porosities. In the interval under consideration (108.0–397.8 mbsf), the log porosities exhibit virtually no evidence of a compaction trend, in contrast to the evidence from both core porosities and log velocities. This discrepancy is caused by the assumption of constant formation-water resistivity, implicit in the calculation of porosity from resistivity. Increased temperature with increasing depth causes a decrease in formation-water resistivity, obscuring the effect of compaction on measured resistivity (Jarrard et al., in press). Unfortunately, temperatures near the borehole are disturbed by drilling and are difficult to predict.

Sonic log velocities range from about 1.4 km/s to 1.8 km/s between 108.0 and 343.0 mbsf, showing generally very low amplitudes. A comparison of laboratory and log compressional wave velocities is also hampered by coring disturbance (Fig. 5). The laboratory samples did not exceed the velocity of water until Core 113-693B-3X (240.0 mbsf). Log-derived velocities are 50–150 m/s higher than those from the laboratory measurements. We consider the log velocities to be accurate, based on consistency of replicate measurements and on the match between a log-based synthetic seismogram and the seismic section across the site (Shipboard Scientific Party, 1988b). Rebound causes the laboratory velocity measurements to be lower than log measurements. The effect of rebound is much higher on velocity than on porosity because of reduction in dynamic rigidity (Hamilton, 1979; Fulthorpe et al., 1989).

Both laboratory and log porosities for Site 693 are generally 5–10 porosity units higher than the average porosity/depth trend for terrigenous sediments (Hamilton, 1976). Moreover, the log velocities are about 0.1 km/s slower than the average velocity/depth trend for terrigenous sediments (Hamilton, 1979). In both cases, the difference is likely to be attributable to substantial diatom content of the sediments at Site 693. Because of high intragranular porosity, even a modest diatom content causes a substantial increase in porosity and decrease in velocity (e.g., Jarrard et al., in press).

Superimposed on the broad-scale compaction-related trends in porosity and velocity are small-scale fluctuations. These fluctuations are barely visible on large-scale plots such as Figure 2, but they are quite evident on expanded-scale plots such as Figure 6. Examination of interlog relationships over short intervals can reveal the geologic cause of these small-scale fluctuations. In a subsequent section we will consider the possibility that

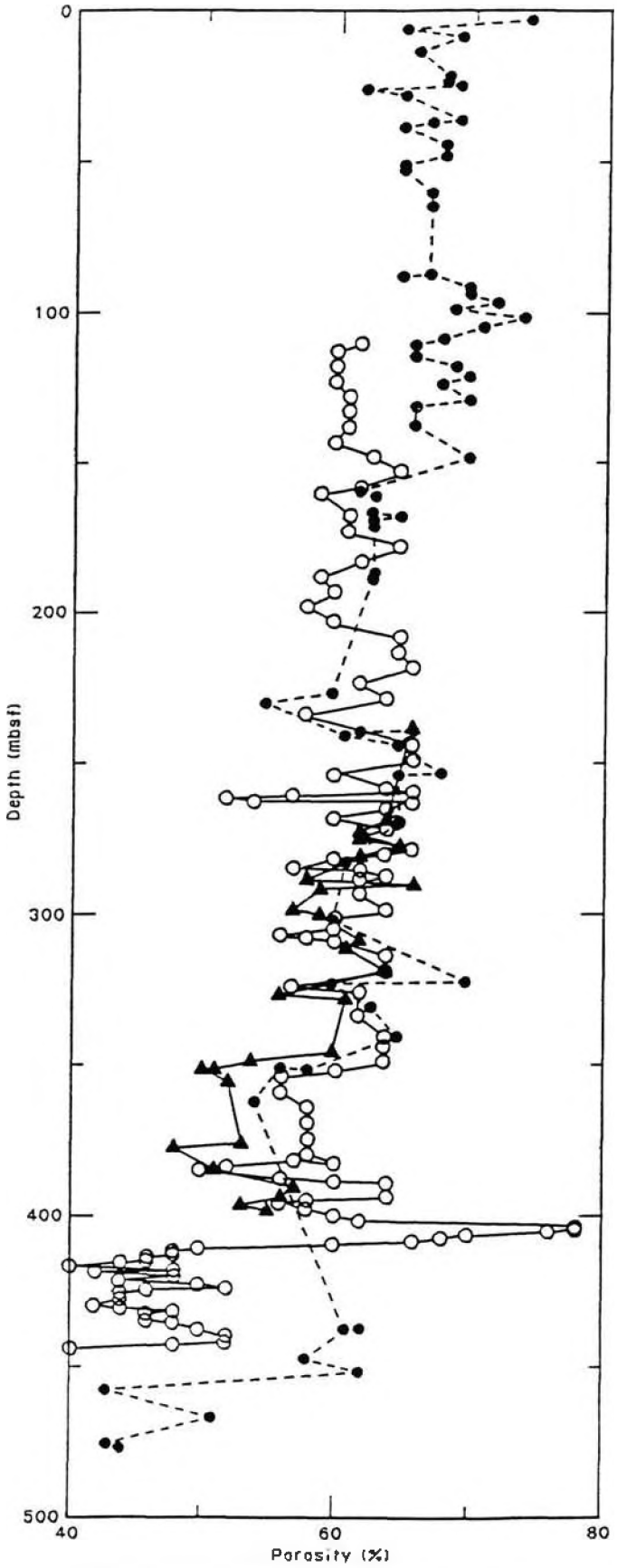

Figure 4. Comparison of porosity measurements from discrete samples (closed circles: rotary cored samples from Hole 693A, and triangles: XCB cored samples from Hole 693B) with porosities determined from the resistivity log (open circles)(from Shipboard Scientific Party, 1988b).

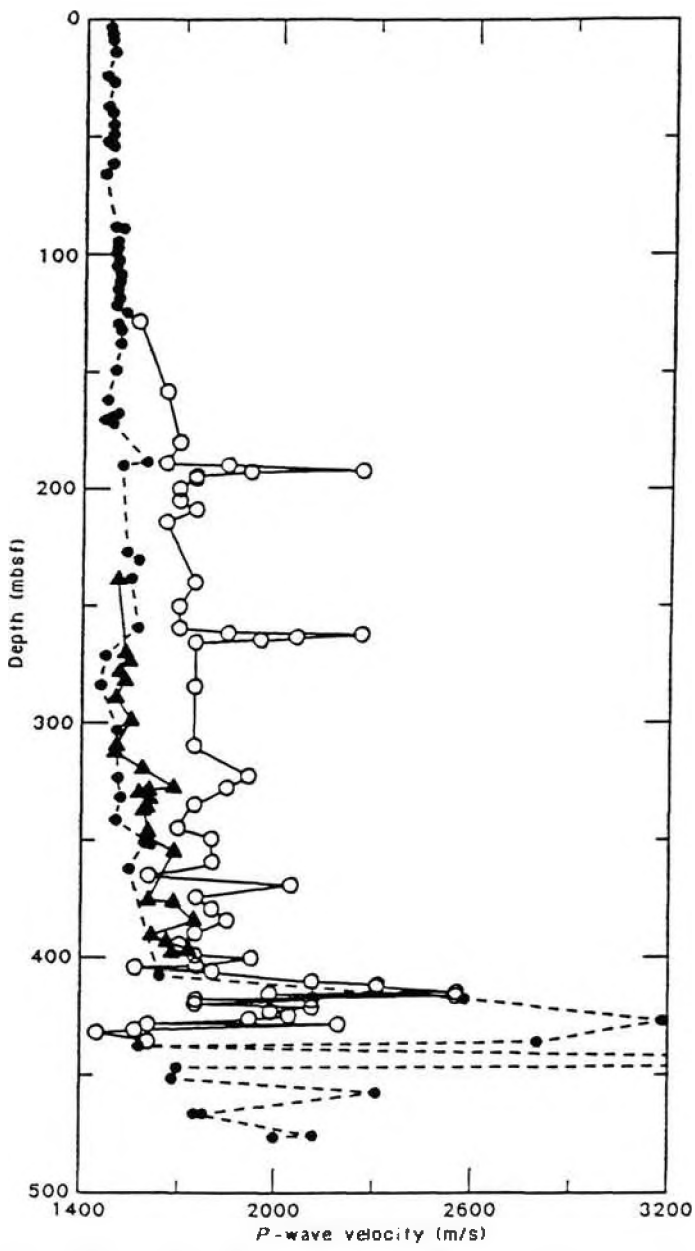

Figure 5. Comparison of laboratory determined compressional wave velocity (closed circles = RCB samples from Hole 693A; triangles = XCB samples from Hole 693B; all measurements made on the Hamilton Frame) with downhole logging velocities (open circles). Although the absolute values are different, both types of measurements display similar trends (from Shipboard Scientific Party, 1988b).

these fluctuations have Milankovitch periodicities with paleoceanographic implications.

As seen in the log interval of Figure 6, small-scale fluctuations in resistivity and velocity are correlated. By calculating the correlation coefficient between the sonic and shallow-focused resistivity logs over short 10-m intervals (Fig. 7), we see that this correlation is not confined to the interval of Figure 6 but extends throughout the logged interval. Such a correlation confirms that velocity and resistivity fluctuations at Site 693, like those in almost all high-porosity sediments, primarily reflect porosity fluctuations. Indeed, the correlation is usually much higher than in the shallowest logged interval of Figure 7, because velocity is relatively insensitive to porosity at extremely high porosities (Raymer et al., 1980).

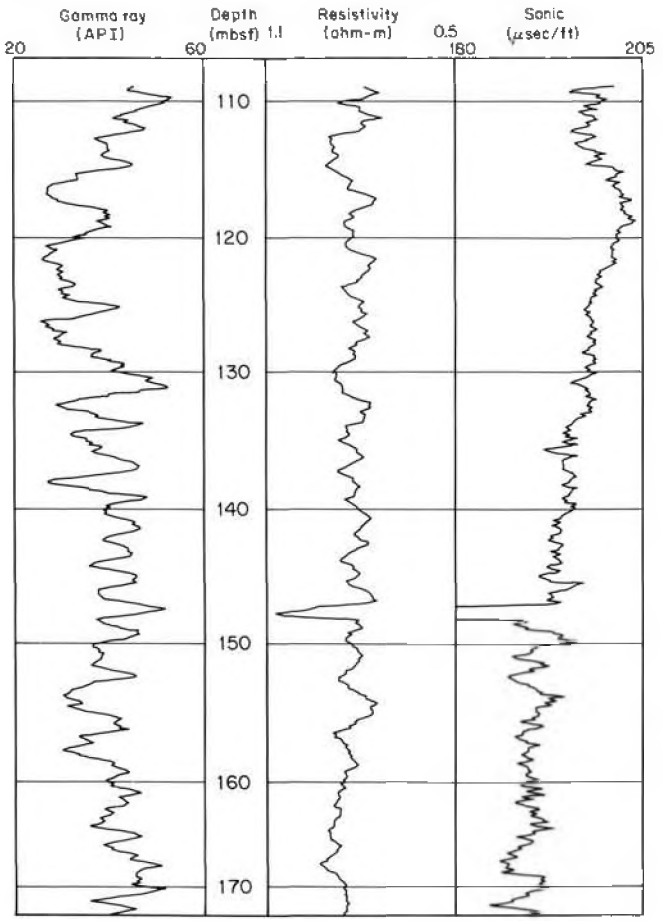

Figure 6. Plots of gamma-ray, resistivity, and sonic logs for the depth interval 108.0–172.0 mbsf, with scales expanded to show the small-scale cyclicity of all three logs.

The two components that have the most dramatic effect on porosity are clay minerals and diatoms. Both are present at Site 693, and we have already inferred that diatoms influence the compaction trends at the site. We can estimate whether diatom or clay content has the greater impact on the porosity fluctuations at this site by examining correlation coefficients of gamma-ray logs with resistivity and sonic logs. If clay fluctuations are dominant, one expects gamma-ray peaks (high clay content) to correlate with resistivity troughs and sonic peaks (high porosity). In contrast, if diatom fluctuations are dominant, one expects the opposite correlation, because diatoms will dilute clay content and therefore reduce gamma-ray counts.

At Site 693 gamma ray is positively correlated with resistivity and inversely correlated with sonic (Fig. 7) throughout the interval 108.0–261.0 mbsf, indicating that diatom abundance fluctuations control the variations in all three logs. Below 261.0 mbsf the correlation is much more variable, and it is likely that in different intervals either diatom or clay-content fluctuations may locally dominate small-scale log responses.

Hard Layers

At least six velocity spikes are evident on the sonic log of Figure 2, at 148.0, 191.5, 261.0–263.5, 284.3–285.8, 322.0, and 368.5 mbsf. These thin layers with very high velocity are confirmed to be real by their presence on both sonic traveltime logs and, in five cases, on the resistivity logs (Fig. 8). Amplitudes of these "hard streaks" are lower on the resistivity logs than on the sonic logs because of lower vertical resolution in the former. In general, the thicker hard streaks have higher velocity and resistivity log responses than do thinner ones, because of the thin-bed effect of vertical resolution.

The hard streaks may be caused by highly cemented or dropstone-rich horizons; they were not recovered in cores. They show no consistent correlation with gamma-ray variations (Fig. 8), though the composition of most of the dropstones analyzed from Site 693 (Shipboard Scientific Party, 1988b) would suggest high potassium concentrations and therefore high gamma-ray values. There is no evidence of a sudden porosity increase (resistivity decrease and sonic traveltime increase) beneath the hard streaks as would occur if cemented, laterally continuous hard streaks acted as a permeability barrier to the expulsion of interstitial water. Indeed, a porosity decrease is sometimes evident (Fig. 8), possibly indicating a sudden compaction increase associated with eroded missing section. The thickest of these hard streaks occurs at 261.0–263.5 mbsf and corresponds to a major micropaleontological unconformity (Shipboard Scientific Party, 1988b). It is possible that the other hard streaks also indicate unconformities or condensed sections, marked by either increased dropstone occurrence or diagenesis at the seafloor. However, the age data for Site 693 (Shipboard Scientific Party, 1988b) lack the precision to either confirm or reject this possibility. Lacking further constraints, the hard streaks remain an enigma. The velocity spikes can have a disproportionately large effect on spectral analysis and therefore were replaced by a constant value prior to spectral analysis.

Spectral Analysis Techniques

Small-scale cyclicity is pervasive in all three log types from Site 693. Although not apparent at the scale of depth plots encompassing the entire logged interval (Fig. 2), this cyclicity is evident on expanded plots of short intervals (e.g., Fig. 6). When more than one frequency is present in a time series such as these log/depth plots, spectral analysis is often superior to a time series plot for identification of the relative strengths of different frequencies. Therefore the log data were converted from the depth domain to the frequency domain via spectral analysis.

Prior to spectral analysis a first-degree regression trend was removed from each 256-point log interval, and the log interval was standardized. This step eliminates the zero-order term, associated with the non-zero mean of the log data, which would otherwise dominate the amplitude spectrum. It also reduces the effect of gradual trends such as compaction on the spectra. Standardization assures numerical stability in the calculation and causes the vertical axis of each spectrum to be percent of total variance. A Hanning filter was applied to each spectrum. The sample spacing is smaller than the vertical resolution of the logs. This may induce a slight spectral contamination at frequencies near the Nyquist frequency, well beyond the frequencies of interest here.

Reconnaissance spectral analysis was performed on the resistivity and sonic logs in two separate depth intervals: 108.0–245.0 mbsf (Fig. 9) and 261.0–337.0 mbsf (Fig. 10). Spectral analysis was not attempted on the gamma-ray curve because of the lower signal-to-noise ratio of this log compared to the sonic and resistivity. The break between the two intervals chosen corresponds to a distinct change in the gamma-ray baseline and spikes in velocity and resistivity, associated with a major unconformity and change in sedimentation rates. The lower limit of the second interval, 337.0 mbsf, was chosen because of poor control on sedimentation rates on the logged interval below this depth. Between 343.0 and 397.0 mbsf, the sediments show evidence of slumping, scouring, and/or current winnowing, which would obscure cyclic sedimentary patterns. Below 397.8 mbsf, in the lower Cretaceous sediments, the age control is too poor to

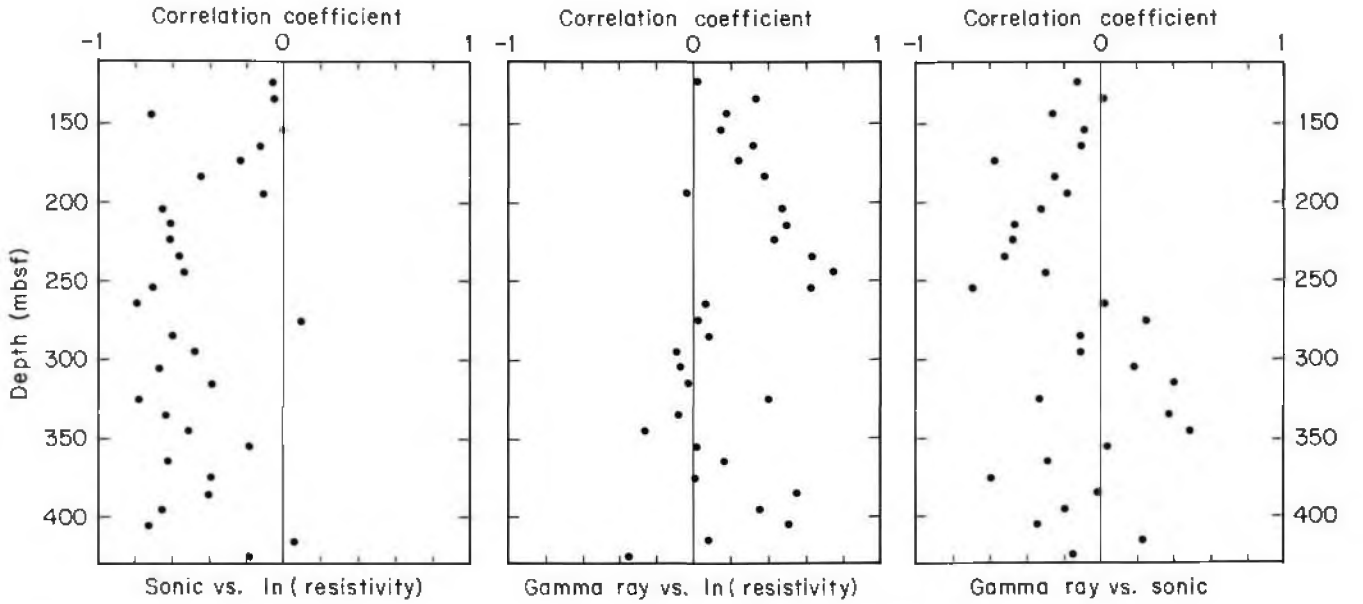

Figure 7. Correlation coefficients between gamma ray, resistivity, and sonic logs, calculated for 10-m intervals. Note the consistent inverse correlation between sonic and resistivity, attributed to porosity control on both logs. Note also the correlation between gamma-ray and these two porosity-sensitive logs, attributed to diatom variations as a control of porosity fluctuations.

establish any sedimentation rates. Possible implications of the cyclicities evident in Figures 9 and 10 are discussed in subsequent sections.

Milankovitch Cycles and Logs

Changes in the earth's orbital parameters control important cyclic variations in global and regional climate and in oceanographic processes (Hays et al., 1976). The spectral analyses of this study were undertaken to see if frequency variations in the well logs of early Pliocene through late Oligocene age collected at ODP Site 693 reflect the influence of changes in the earth's orbital parameters, and which features of the sediment column (e.g., lithology, velocity, porosity) were the most affected. Although the "Milankovitch periods" of precession (19,000–23,000 yr), obliquity (41,000 yr), and eccentricity (95,000–123,000 and 413,000 yr) are most commonly described in Pleistocene deep-sea sediments (e.g., Hays et al., 1976; Imbrie et al., 1984; Ruddiman et al., 1986), they have also been observed in a wide variety of sedimentary sequences of many different ages. For example, they have been observed in Cretaceous chalk/shale sequences (Arthur et al., 1984; Fisher and Schwarzacher, 1984) and Triassic lake sediments (Olsen, 1986), and thus the climatic influence does not appear to be restricted to either the deep-sea or to the Pleistocene. The Pleistocene bias is a combination of very strong glacial/interglacial climatic fluctuations, of high-resolution dating, and of availability and ages of deep-sea piston cores.

In pelagic deep-sea sediments $\delta^{18}O$ of biogenic carbonate (an indicator of ice volume and paleotemperature) and calcium carbonate concentration (an indicator of the balance between paleoproductivity, dissolution, and/or dilution by other components) are the parameters most commonly measured to detect Milankovitch frequencies. Sedimentary responses to Milankovitch forcing, however, are detectable in a wide variety of parameters which are commonly measured (Fig. 11). Sedimentary responses can be expected to differ as a function of time at one location and between regions receiving different sediment supplies. For example, cycles of surface temperature or upwelling may cause variations in one or more biogenic components in one region, while aridity/humidity cycles or variations in bottom-current strength or ice-rafted material may cause detectable fluctuations in clay mineralogy or clay abundance in another region. Thus consideration of both mineralogical and porosity fluctuations is necessary for a comprehensive analysis of Milankovitch cycles in any sedimentary sequence.

Downhole geophysical logs can be used to detect periodic changes in mineralogy (gamma-ray log), porosity (resistivity log), and velocity (sonic log) associated with orbital changes (Fisher, 1986). Downhole logs have four principal advantages over core analyses for the detection of Milankovitch frequencies. First, log measurements are continuous and are independent of core recovery. In general, ODP core recovery decreases from around 94% in the upper 150 m of the sediment column to 50%–60% below 200 mbsf, provided that no "difficult" sediments such as sand or shallow-water carbonates are encountered. This poor recovery limits the detection of Milankovitch cycles in pre-Pleistocene ODP cores and creates uncertainty about the original depths of the recovered material. In addition, in some cores the sediments are completely homogenized by coring (rotary coring) while in others, up to 50% of the core consists of drilling slurry interbedded with small biscuits (extended core barrel). Second, almost any significant periodic change in porosity and mineralogy is detectable with the variety of geochemical and physical properties measured (Fig. 11), provided that sedimentation rates are high enough to allow resolution of the cycles by the logging tools. Third, logging is much faster than discrete core analyses. And, fourth, identification of cycles in sedimentary material commonly depends on there being a distinct lithologic expression (e.g., color changes) and the cycles occurring within one core length (i.e., not more than 10 m).

Problems, however, are also encountered with the detection of Milankovitch frequencies in downhole logs. Some of these problems are the same as for cores. For example, good age control for an accurate conversion from frequencies in depth to temporal frequencies is necessary for both cores and logs. Cycles in either cores or logs can be caused by local sedimentary deposition (autocyclic), such as turbidites, as well as regional

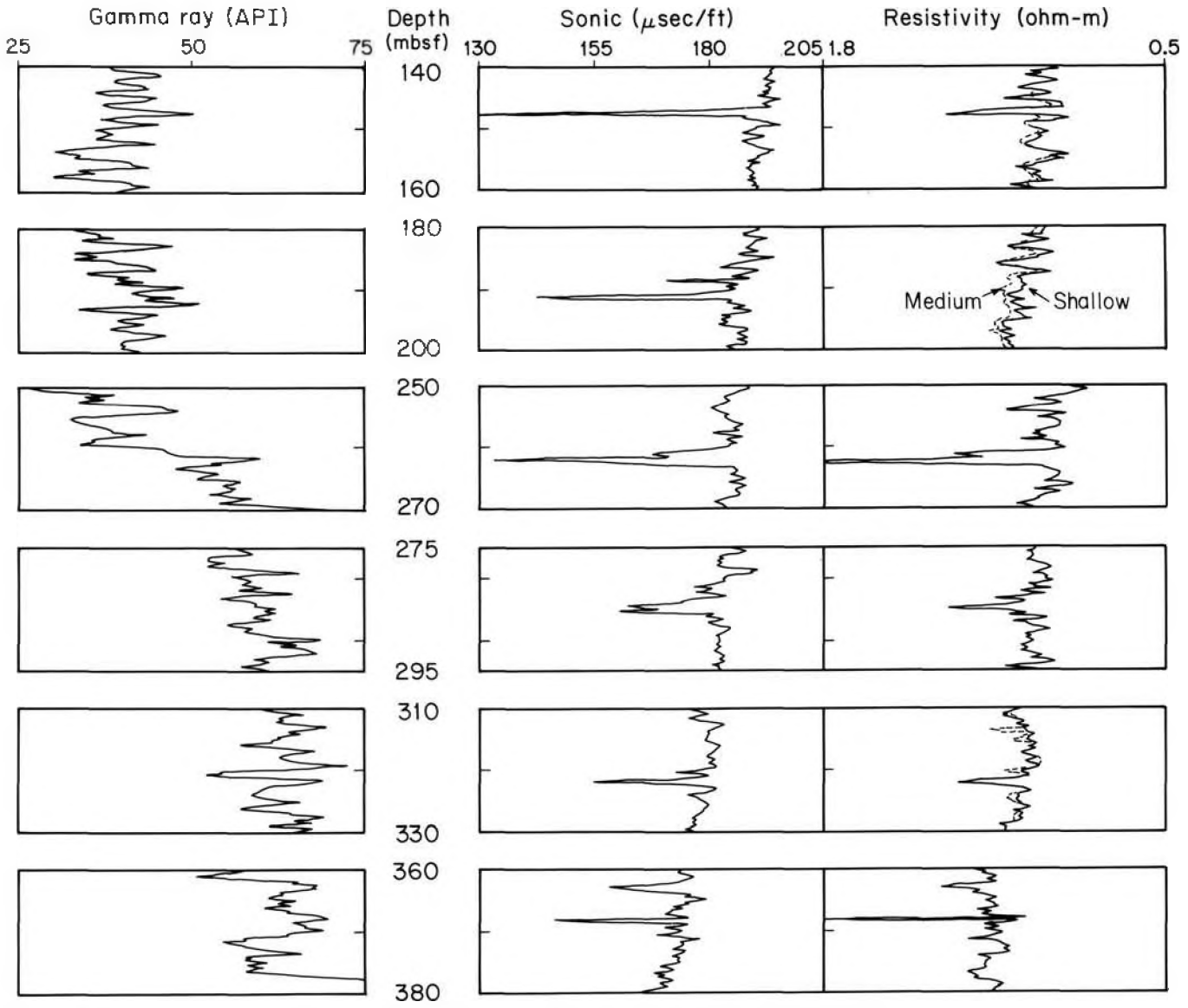

Figure 8. Detail of log variations bracketing six "hard streaks," or thin, high-velocity, high-resistivity zones.

climatic or oceanographic (allocyclic) changes. Distinguishing the type of cyclicity requires the combined effort of studying both cores and logs.

In addition there are problems in distinguishing Milankovitch frequencies that are unique to logs. Vertical resolution is the major limitation, in that only cycles with wavelengths greater than 2 m are detectable, a problem which becomes particularly acute during periods of low sedimentation. A second, although minor, limitation is that logs measure the indirect effects of climatic change (e.g., porosity and mineralogical change) rather than the direct effects (e.g., changes in water temperature).

Possible Milankovitch Periods at Site 693

The predicted location of specific Milankovitch frequencies on the amplitude spectrum is determined by:

[window length (m)/sedimentation rate (m/m.y.)]/orbital frequency = predicted frequency (1.1)

where the window length is a depth interval 2n samples long, the sedimentation rate is taken from the published shipboard sedimentation rate (Shipboard Scientific Party, 1988b), and the orbital frequency is one of the Milankovitch frequencies. Sedimentation rate estimates were based on a combination of biostratigraphic zonations (particularly diatom and radiolarian) with shipboard magnetostratigraphy, using the timescale of Berggren et al. (1985a and b).

The presence or absence of the different predicted peaks is variable for the different depth windows. In part this may be attributed to the vertical resolution of the different logs: 0.46 m for the gamma-ray tool, about 1.2 m for the resistivity tool, and 0.6 m for the sonic tool (Allen et al., 1988). These resolutions correspond to different critical temporal resolutions depending on the sedimentation rate (Table 1). Average shipboard sedimentation rate estimates range from 50 m/m.y. to 8 m/m.y.

Unit 1 (108.0–245.0 mbsf)

The amplitude spectra for the sonic and resistivity logs for this lower Pliocene to upper Miocene unit are displayed in six different 39-m-long depth windows (Fig. 8). To avoid abrupt changes, there is a 50% depth overlap between adjacent windows. The presence and resolution of peaks are variable among

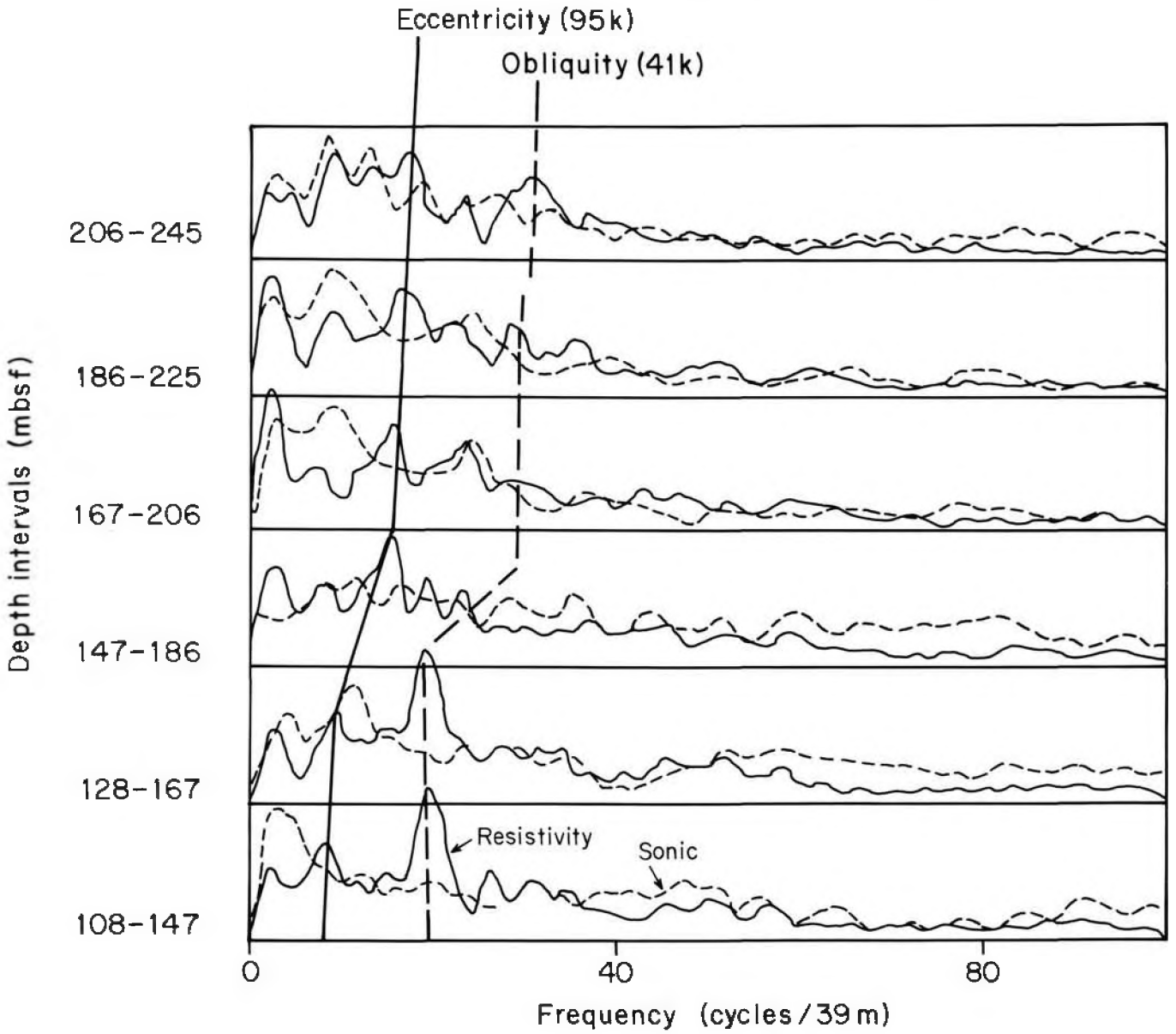

Figure 9. Resistivity and sonic amplitude spectra for the interval 108.0–245.0 mbsf, shown in six overlapping 39-m intervals. Vertical scale of amplitude spectra is percent of total variance. Assuming an average sedimentation rate of 32.2 m/m.y., orbital periods should occur as follows: 41,000 yr at 29.5; 95,000 yr at 12.8; 125,000 yr at 9.6; and 410,000 yr at 3. Since the positions do not line up perfectly, a dashed line connects an estimate of the frequency peak location for each successive interval. The adjusted location of the peaks is used to calculate the derived sedimentation rates given in Tables 3 and 4.

the different logs and are not necessarily compatible. In none of the spectra do amplitude peaks correspond well to the shipboard average sedimentation rate of 32 m/m.y. for the interval.

To cope with the problem of uncertain and variable sedimentation rates within Unit I, we used a three-step procedure. First, we calculated sedimentation rates between datum pairs on the shipboard age/depth curve. The age determinations are, at best, accurate to ± 0.5 m.y. This sedimentation rate estimate was used to predict locations of potential Milankovitch peaks on the spectra. Second, we tentatively assumed that the dominant peak on the resistivity log is a Milankovitch peak, and we used the frequency at which it occurred to determine both a slightly revised sedimentation rate and the revised predicted locations of the other Milankovitch frequencies. Third, we determined whether the predicted locations of other peaks corresponded to observed locations. Only if this third step is successful does one avoid the trap of forcing a Milankovitch interpretation on poorly constrained data.

The first two intervals, 108.0–147.0 mbsf and 128.0–167.0 mbsf (lower Pliocene), have very similar spectra. Assigning the highest peak to 41,000 yr gives a sedimentation rate of 50 m/m.y. and an excellent correlation with the other Milankovitch frequencies. Location of the Milankovitch frequency peaks is given in Table 2, and the quality of the correlation of the Milankovitch frequencies with major peaks from the well-log spectrum is given in Tables 3 and 4. At this sedimentation rate, the 41,000-yr peak should be marginally identifiable on the resistivity log.

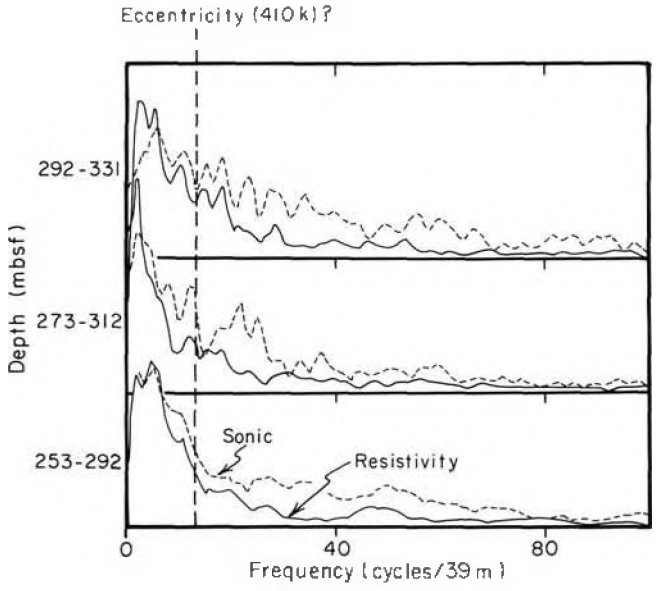

Figure 10. Resistivity and sonic amplitude spectra for the interval 253.0–331.0 mbsf, shown in three overlapping 39-m intervals. Vertical scale of amplitude spectra is percent of total variance. Assuming an average sedimentation rate of 8 m/m.y., orbital periods should occur as follows: 125,000 yr at 39 and 410,000 yr at 12. A dashed line indicates the predicted location of the 410,000-yr period; note that this period is weak or absent (Table 4).

The lowermost three intervals, 166.0–206.0 mbsf, 186.0–225.0 mbsf, and 206.0–245.0 mbsf, have much lower sedimentation rates of about 26 m/m.y. according to the shipboard sedimentation rate curve. At these low rates, we would not expect a 41,000-yr signal to be detectable. Instead, the high peak near 15 (cycles/39 m) would approximately correspond to the 95,000-yr cyclicity.

The 147.0–186.0 mbsf interval has a mixed signal. The dominant peak, at 15 (cycles/39 m), could represent a 41,000-yr cyclicity if 65 m/m.y. is the sedimentation rate, or a 95,000-yr cyclicity if 26 m/m.y. is the sedimentation rate. Since this interval is a combination of a 50 m/m.y. and a 26 m/m.y. sedimentation rate, it is not possible for it to have a higher sedimentation rate. We therefore think that the 26 m/m.y. sedimentation rate is the best approximation and that some of the adjacent peaks are indicative of signal mixing. All the peaks are better defined on the resistivity frequency spectrum than on the sonic frequency spectrum. Since the sonic log is affected by changes in both porosity and lithology, the frequency response implies that the changes in both parameters are not synchronous and are probably controlled by different factors.

Unit 2 (253.0–331.0 mbsf)

Shipboard sedimentation rates for this unit are about 8 m/m.y. At these low rates, only the 410,000-yr peak should be identifiable, if present, on the resistivity spectrum (Table 1). With only one peak even potentially detectable, no confirmation is possible that any peak represents a Milankovitch frequency. As expected for such a low sedimentation rate, no single peak is dominant.

SEDIMENTOLOGIC AND PALEOCEANOGRAPHIC IMPLICATIONS

In this section we will discuss the mineralogical and paleoceanographic factors controlling both cyclical and long-term porosity changes in the logged interval. In these cores, porosity variations, usually attributed to grain size changes, are instead attributed primarily to variations in the abundance of biosiliceous sediments. Even minor increases in diatom and/or radiolarian content can produce measurable porosity increases (Shipboard Scientific Party, 1988b; Jarrard and Arthur, in press; Bryant and Rack, this volume). Although lithologic variation in the logged interval is minor, it does dominate the gamma-ray response and cause much of the observed difference between sonic and resistivity logs.

261.0–348.0 mbsf (late Oligocene to late Miocene)

The upper Oligocene to upper Miocene section from 261.0–348.0 mbsf (Unit IV, Subunit IIIC) appears to have the lowest average sedimentation rate examined in this study (8 m/m.y.) and is bracketed by hiatuses. This was a period of low to moderate biosiliceous productivity with considerable opal dissolution, so other short duration hiatuses may also exist (Shipboard Scientific Party, 1988b). In addition to the major hard streak at 261.0–263.5 mbsf that marks the hiatus capping this interval, hard streaks are also observed on the logs at 284.3–285.8 and 322.0 mbsf. Included in the interval are many reworked diatoms, implying downslope transport. Among these downslope contaminants are benthic diatoms, suggesting an ice-free coastal environment (Shipboard Scientific Party, 1988b).

The hiatus at 261.0 mbsf marks the largest Cenozoic change in gamma-ray response, a significant drop in the gamma-ray baseline. Clay minerals below 261.0 mbsf consist dominantly of illite, with minor smectite and kaolinite, reflecting the predominance of physical erosion (Shipboard Scientific Party, 1988b). Above the unconformity chlorite and kaolinite are more common than below it. The sudden drop in gamma ray is probably caused primarily by a decrease in the proportion of potassium-rich illite. The drop may also be partly due to a drop in total clay minerals, a continuation of the trend of decreasing clay content noted in cores and confirmed by the gamma-ray log for the interval 290.0–261.0 mbsf.

Sedimentation rates in this interval were too low, and probably too intermittent, to allow the determination of high resolution Milankovitch frequencies. With only the 410,000-yr peak potentially detectable and with many small peaks rather than a single dominant peak (Fig. 7), frequency analysis is not possible.

167.0–261.0 mbsf (late Miocene to early Pliocene)

Between 167.0 and 261.0 mbsf (Subunit IIIB and part of Subunit IIIA), sedimentation rates averaged 26 m/m.y. The gamma-ray log shows this sediment to have a lower clay content and to be more variable than the lower interval. The log-derived porosity values are also variable, ranging from about 55 to 65% and showing two decreasing trends in the intervals 175.0–200.0 mbsf and 215.0–235.0 mbsf. The upper decrease in porosity corresponds to a decrease in diatom content. A decrease is not as apparent in the lower interval, except in its lower portion, which terminates in a silty mud with very low diatom content. As previously discussed, interlog relationships in the interval 167.0–261.0 mbsf indicate that diatom fluctuations are responsible for most of the variations on all three logs.

These diatom fluctuations have a regular, strong periodicity that may correspond to the 95,000–123,000-yr period of eccentricity. At sedimentation rates of 26 m/m.y., cyclic variations less than 92,000 yr long would not be detectable with resistivity, and therefore only eccentricity could be detected (Table 3). The spectra for this interval (Fig. 8) show a strong resistivity peak at 95,000 yr, but there are also several adjacent peaks that might be equally valid, if a different sedimentation rate were assumed. Spectra from the sonic logs do not correspond to either the ec-

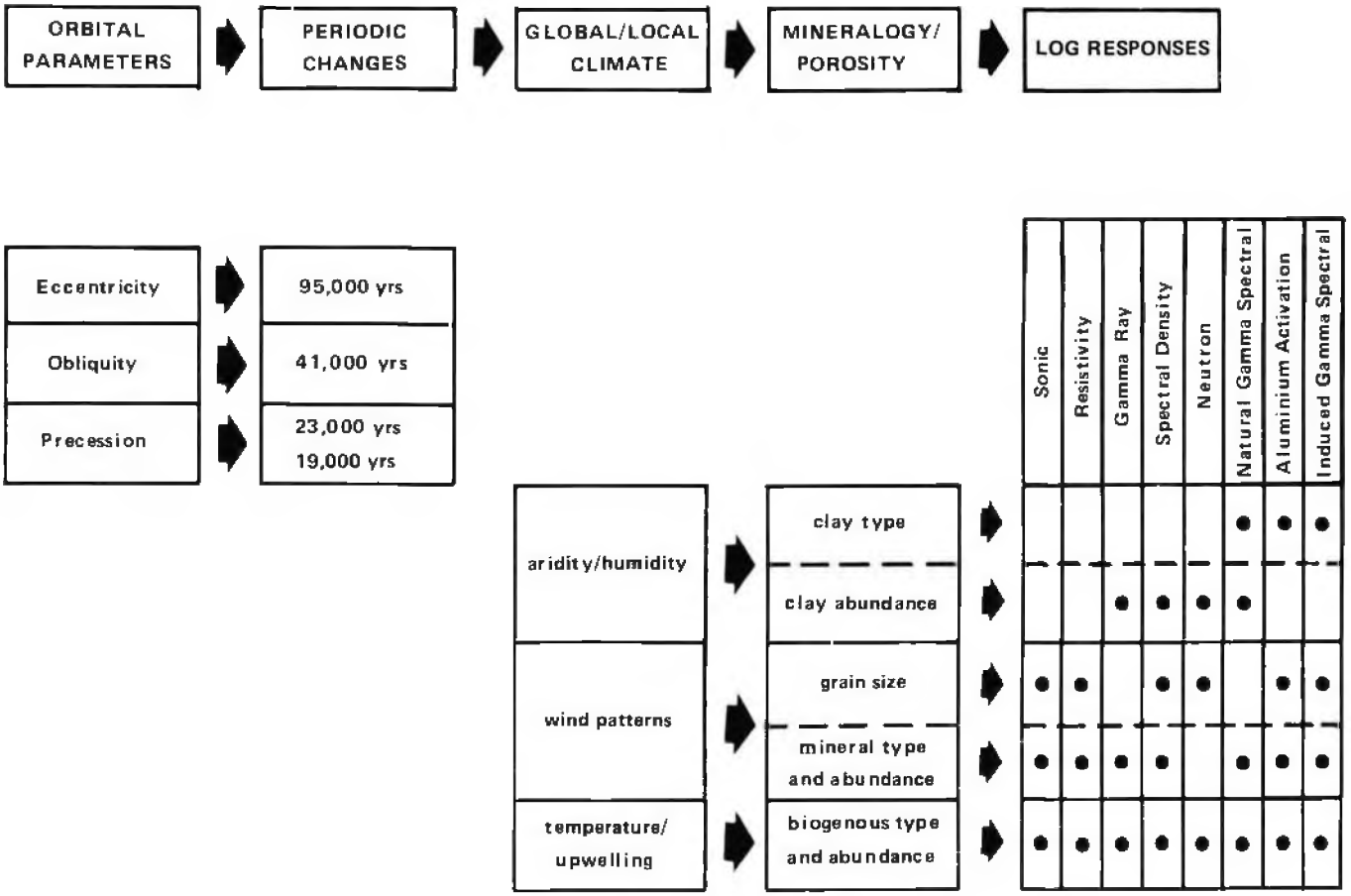

Figure 11. Flow chart of possible climatic effects on geophysical logs. Climatic fluctuations, whether associated with periodic changes in orbital parameters or with local climate, are likely to cause fluctuations in mineralogy or porosity of deep-sea sediments. If so, then these mineralogic or porosity changes are usually detectable in geophysical logs; the affected log depends on the type of mineralogic or porosity change and therefore indirectly on the type of climatic change affecting the sediments (from Jarrard and Arthur, in press).

Table 1. Maximum vertical well-log resolution for the three types of logs run at Site 693.

Sedimentation rate (m/m.y.)	Gamma ray 0.46 m res. (yr)	Resistivity 1.2 m res. (yr)	Sonic 0.6 m res. (yr)
8	120,000	300,000	150,000
26	35,000	92,000	46,000
32	30,000	74,000	37,000
50	18,000	48,000	24,000
98	9,000	24,000	12,000

Table 2. Location of Milankovitch frequency peaks using assumed sedimentation rates.

Sedimentation rate[a] (m/m.y.)	Milankovitch frequencies[b] (ky) 410	125	95	41	23	19
50	1.9	6.2	8.2	19.0	33.9	41.0
26	3.6	12.0	15.8	36.6	–	–

[a] Sedimentation rate determined by assigning highest peak to 41,000 or 95,000 yr, measuring the frequency at which it occurs, and using equation 1.1 to determine sedimentation rate.

[b] Milankovitch frequency intervals determined with equation 1.1 using the assigned sedimentation rate.

centricity or the obliquity peaks. For this interval, the low sedimentation rates render this method for determining Milankovitch frequencies invalid.

Near the base of this unit, between 243.9 and 253.6 mbsf in cores, the carbonate content increases to 7%. Because of the difficulty in exactly correlating well logs and cores, it is not clear where the 130 cm interval of most carbonate-rich sediment lies relative to the logged interval. The strong inverse correlation between gamma ray and porosity in this zone clearly indicates that it is characterized by alternations of diatomaceous clay and clayey diatomite, with perhaps the most diatomaceous sediments of the entire site occurring at 248.0 and 251.0 mbsf. Based on core evidence that the most nannofossil-rich sediments in this interval are also higher in diatoms, these two horizons are probably rich in nannoplankton. The interval 244.0–254.0 mbsf, and in particular the log-based horizons at 248.0 and 251.0 mbsf, has the highest carbonate content recovered in the Cenozoic section of the core, consisting of moderately to well preserved benthic foraminifers and nannofossils. The dominant diatom within this interval, *Denticulopsis dimorpha*, is associated with cold climatic conditions elsewhere in Antarctica (L. Burckle, pers. comm.), and therefore, contrary to some interpretations (e.g., Corliss and Thunnell, 1983; Grobe, 1986), this layer is believed to represent an early late Miocene cooling event.

These data suggest a general early Oligocene to early Miocene cooling trend, with increased carbonate productivity near

Table 3. Quality of match between calculated Milankovitch frequency peak using sedimentation rates given in Table 2, with location of actual peak given in Figure 8, for interval 108.0–245.0 mbsf.

Depth (mbsf)	Milankovitch frequency interval[a] (ky) 410	95	41	23	19	Log type
108–147	G	G	M	P	P	Resistivity
(50 m/m.y.)	G	P	P	P	P	Sonic
128–167	G	G	G	G	P	Resistivity
(50 m/m.y.)	M	M	P	M	P	Sonic
147–186	G	G	P	P	P	Resistivity
(26 m/m.y.)	P	P	P	M	P	Sonic
167–206	G	G	P	–	–	Resistivity
(26 m/m.y.)	M/P	P	P	–	–	Sonic
186–225	G	P	G	–	–	Resistivity
(26 m/m.y.)	G	P	P	–	–	Sonic
206–245	G	M/P	G	–	–	Resistivity
(56 m/m.y.)	G	M/P	P	–	–	Sonic

[a] Quality of interval frequency is determined by the presence or absence of the top or near top of an amplitude peak within ± 0.5 m.y. of the predicted frequency. Correlation: G = good, M = moderate, P = poor. Table 2 gives the predicted frequency location.

Table 4. Quality of match between calculated Milankovitch frequency peak using the sedimentation rate given in Table 2, with the location of the actual peak given in Figure 9, for the interval 253.0–331.0 mbsf.

Depth (mbsf)	Milankovitch frequency interval[a] (ky) 410	125	Log type
253–292	G	G	Gamma ray
	P	P	Resistivity
	P	P	Sonic
273–312	P	M	Gamma ray
	G	P	Resistivity
	G	P	Sonic
292–331	M	M	Gamma ray
	P	M	Resistivity
	M	M/P	Sonic

[a] Quality of interval frequency is determined by the presence or absence of the top or near top of an amplitude peak within ± 0.5 m.y. of the predicted frequency. Correlation: G = good, M = moderate, P = poor. Table 2 gives the predicted frequency location.

the base of the unit. The strong cyclicity of diatom fluctuations throughout this interval may have resulted from increased upwelling and bottom currents associated with climatic deterioration and probable ice buildup. During the Langhian (early middle Miocene) there are two fairly major sea-level falls (Haq et al., 1987), and these are close to the time of the 261.0 mbsf hiatus. The hiatus may be correlated with the sea-level fluctuations, especially if the fluctuations are caused by the build-up and melting of Antarctic ice sheets.

Illite decreases uphole in this interval (167.0–261.0 mbsf) while chlorite and kaolinite increase. The chlorite abundances in particular may reflect the increased removal of chlorite from Antarctica, possibly during a slight deglaciation. A late Miocene warming was recorded in the southwest Pacific (Kennett and Von der Borch, 1986), and associated increases in chlorite were observed on the Falkland Plateau (Robert and Maillot, 1983). However, such increases were slight at Site 689 on the Maud Rise (Shipboard Scientific Party, 1988b; Robert and Maillot, this volume). The sand-sized sediment tends to be poorly sorted and is most likely derived from melting ice.

These data suggest that, during the late Miocene to early Pliocene, Antarctica experienced a general cooling, but the cooling trend lessened in the late Miocene.

108.0–167.0 mbsf (early Pliocene)

The interval from 108.0 to 167.0 mbsf (upper part of Subunit IIIA) has the highest sedimentation rate in this study and fairly constant log porosity values of around 60%. Diatom percentages are again fairly constant but show gradual variations of about 30%. These variations are reflected by a consistent correlation of high-porosity log responses (low resistivity and high sonic traveltime) with low clay content (low gamma ray).

With sedimentation rates of only 50 m/m.y., the high-frequency precession period cannot be detected, but both the obliquity and eccentricity periods are well represented on the resistivity log (Fig. 8, Table 3). The positive correlation of these porosity changes with Milankovitch frequencies suggests that Antarctic climatic changes in the early Pliocene were influenced by orbital forcing.

This interval lies within clay mineral unit C1 (Shipboard Scientific Party, 1988b; Robert and Maillot, this volume). The smectite-rich clay unit suggests removal of ancient smectite-rich sediments from the Antarctic continental margin, which is thought to occur during colder periods. The smectite percentage varies by as much as 30%, usually replaced by illite. Near Kapp Norvegia, this alternation is attributed to warm (smectite/montmorillonite poor) and cold (smectite/montmorillonite rich) periods, suggesting alternating climatic conditions. These alternations correspond to productivity changes with higher biogenic silica contents occurring during the warmer periods (Grobe, 1986). The very large gamma-ray swings (Fig. 6) could be caused by the alternation between potassium-rich illite and potassium-poor smectite. However, the previously mentioned correlation of gamma ray with porosity would then imply that high diatom abundance is associated with smectite rather than illite. Thus, variations in clay abundance, caused by diatom dilution, are probably causing the gamma-ray swings, rather than variations in clay composition. The sand component is unsorted. Unsorted sand is more likely to result from debris flows or ice rafting than turbidite deposition. Since biogenic downslope contamination was not recognized, it is more likely that the sand originated from ice rafting, suggesting that the thermal oscillations (pack ice, shelf ice, and polynya) were occurring within a generally cold period.

CONCLUSIONS

The sediments at Site 693 indicate a gradual climatic deterioration, punctuated by major changes at 261.0 mbsf, the unconformity separating upper and lower Miocene sediments. On both sides of the unconformity, logs indicate that subtle but detectable changes in relative proportions of terrigenous, biosiliceous, and bicarbonate deposition occurred continuously. Below this unconformity, sedimentation rates were low, and no single component dominates the lithologic fluctuations. Above the unconformity, sedimentation rates are higher and diatom variations dominate the log responses. The observed diatom variations could be either primary (productivity) or secondary (dissolution). Productivity changes are caused by the nutrient supply, chiefly influenced by upwelling, which in turn is influenced by variations in the extent of the ice sheet, the pack ice, and the polynya.

The examination of downhole geophysical logs reveals some cyclic variation, particularly in the resistivity log, which records porosity. The porosity-sensitive logs from Site 693 follow a read-

ily explicable pattern of increasing usefulness for Milankovitch analysis with decreasing age. For the lower Oligocene interval 400.0–348.0 mbsf, slumping is pervasive and frequency analysis is inappropriate. For the lower Oligocene–lower Miocene interval 348.0–261.0 mbsf, sedimentation rates are too low (about 8 m/m.y.) and the geologic controls on porosity are too variable for spectral analysis to be meaningful. For the upper Miocene interval 261.0–167.0 mbsf, sedimentation rates of about 26 m/m.y. are sufficient for detection only of eccentricity, and porosity has a simple diatom control. In this interval, a periodicity near to that expected for eccentricity is present. Unfortunately, we cannot confirm that the assumed sedimentation rate is correct by identifying additional Milankovitch periodicities. For the interval 167.0–108.0 mbsf, sedimentation rates are sufficiently high for potential detection of both eccentricity and obliquity. In this interval we see the most convincing evidence of Milankovitch periods in the Site 693 logs, and obliquity is dominant over eccentricity. The observed cycles may represent a gradual change from eccentricity control on diatom abundance to later obliquity control. However, the alternative hypothesis of a sedimentation rate control on our ability to detect obliquity appears more likely.

To confidently identify Milankovitch periods, sedimentation rates must be accurate, relatively high, persist over a sufficiently long depth interval for spectral analysis to be done, and have been determined independent of the assumption that orbitally-induced frequencies are present. In this study sedimentation rates are determined assuming a fairly constant sedimentation rate with no or relatively few hiatuses.

Using the frequency analysis of well logs to derive sedimentation rates suggests that sedimentation rates are variable and/or hiatuses are common. However, the hint of Milankovitch frequencies in the higher sedimentation rate portion of this hole suggests that this method holds promise and should be pursued at other ODP Antarctic sites.

ACKNOWLEDGMENTS

We thank the Shipboard Scientific Party of ODP Leg 113 for the cooperative scientific effort that made this project possible. This manuscript benefited from the reviews of R. Anderson and two anonymous reviewers. Financial support was provided by USSAC.

REFERENCES

Allen, D., Barber, T., Flaum, C., Hemingway, J., Anderson, B., and des Ligneris, S., 1988. Advances in high-resolution logging. *The Technical Review*, 36:4–14.

Arthur, M. A., Dean, W. E., Bottjer, D., and Scholle, P. A., 1984. Rhythmic bedding in Mesozoic-Cenozoic pelagic carbonate sequences: the primary and diagenetic origin of Milankovitch-like cycles. *In* Berger, A., Imbrie, J., Hays, J., Kukla, G., and Saltzman, B. (Eds.), *Milankovitch and Climate, I*: Dordrecht (Reidel), 191–222.

Berggren, W. A., Kent, D. V., and van Couvering, J. A., 1985a. The Neogene: Part 2 Neogene geochronology and chronostratigraphy. *In* Snelling, N. J. (Ed.), *Geochronology and the Geologic Time Scale*. Geol. Soc. London Mem., 10:211–260.

_____, 1985b. Paleogene geochronology and chronostratigraphy. *In* Snelling, N. J. (Ed.), *Geochronology and the Geologic Time Scale*, Geol. Soc. London Mem., 10:141–195.

Corliss, B. H., and Thunnell, R. C., 1983. Carbonate sedimentation beneath the Antarctic circumpolar current during the late Quaternary. *Mar. Geol.*, 5:293–326.

Doveton, J. H., 1986. *Log Analysis of Subsurface Geology—Concepts and Computer Methods*: New York (Wiley).

Fischer, A. G., 1986. Climatic rhythms recorded in strata. *Ann. Rev. Earth Planet. Sci.*, 14:351–376.

Fisher, A. G., and Schwarzacher, W., 1984. Cretaceous bedding rhythms under orbital control? *In* Berger, A., Imbrie, J., Hays, J., Kukla, G., and Saltzman, B. (Eds.), *Milankovitch and Climate, I*: Dordrecht/Boston/Lancaster (Reidel), 163–175.

Fulthorpe, C. S., Schlanger, S. O., and Jarrard, R. D., 1989. In situ acoustic properties of pelagic carbonate sediments on the Ontong-Java Plateau. *J. Geophys. Res.*, 94:4025–4032.

Grobe, H., 1986. Sedimentation processes on the Atlantic continental margin at Kapp Norvegia during the Late Pleistocene. *Geol. Rundsch.*, 75:95–104.

Hamilton, E. L., 1976. Variations of density and porosity with depth in deep-sea sediments. *J. Sediment. Petrol.*, 46:280–300.

_____, 1979. Sound velocity gradients in marine sediments, *J. Acoust. Soc. Am.*, 64:909–922.

Haq, B. U., Hardenbol, J., and Vail, P. R., 1987. Chronology of fluctuating sea levels since the Triassic. *Science*, 235:1156–1167.

Hays, J. D., Imbrie, J., and Shackleton, N. J., 1976. Variations in the Earth's orbit: pacemaker of the ice ages. *Science*, 194:1121–1132.

Imbrie, J., Hays, J. D., Martinson, D. G., McIntyre, A., and Mix, A. C., 1984. The orbital theory of Pleistocene climate: support from a revised chronology of the marine $\delta^{18}O$ record. *In* Berger, A., Imbrie, J., Hays, J., Kukla, G., and Saltzman, B. (Eds.), *Milankovitch and Climate, I*: Dordrecht/Boston/Lancaster (Reidel), 269–271.

Jarrard, R. D., and Arthur, M. A., in press. Milankovitch paleoceanographic cycles in geophysical logs from ODP Leg 105, Labrador Sea and Baffin Bay. *In* Srivastava, S., Arthur, M. A., et al., *Proc. ODP, Sci. Results*, 105: College Station, TX (Ocean Drilling Program).

Jarrard, R. D., Dadey, K. A., and Busch, W. H., in press. Velocity and density of sediments of Eirik Ridge, Labrador Sea: Control by porosity and mineralogy. *In* Srivastava, S., Arthur, M. A., et al., *Proc. ODP, Sci. Results*, 105: College Station, TX (Ocean Drilling Program).

Kennett, J. P., Von der Borch, C. C., et al., 1986. Southwest Pacific Cenozoic paleoceanography. *In* Kennett, J. P., Von der Borch, C. C., et al., *Init. Repts. DSDP*, 90: Washington (U.S. Govt. Printing Office), 1493–1517.

Olsen, P. E., 1986. A 40-million-year lake record of early Mesozoic climatic forcing, *Science*, 234:842–848.

Raymer, L. L., Hunt, E. R., and Gardner, J. S., 1980. An improved sonic transit time-to-porosity transform, *Trans. SPWLA 21st Annual Logging Symp.*, Pap. P.

Robert, C., and Maillot, H., 1983. Paleoenvironmental significance of clay mineralogical and geochemical data, Southwest Atlantic, Deep-Sea Drilling Project Legs 36 and 71. *In* Ludwig, W. J., Krasheninnikov, V. A., et al., *Init. Repts. DSDP*, 71: Washington (U.S. Govt. Printing Office), 317–343.

Ruddiman, W. F., Raymo, M., and McIntyre, A., 1986. Matuyama 41,000-year cycles: North Atlantic Ocean and northern hemisphere ice sheets, *Earth Planet. Sci. Lett.*, 80:117–129.

Shipboard Scientific Party, 1988a. Explanatory Notes. *In* Barker, P. F., Kennett, J. P., et al., *Proc. ODP, Init. Repts.*, 113: College Station, TX (Ocean Drilling Program).

_____, 1988b. Site 693. *In* Barker, P. F., Kennett, J. P., et al., *Proc. ODP, Init. Repts.*, 113: College Station, TX (Ocean Drilling Program).

Date of initial receipt: 1 March 89
Date of acceptance: 10 October 89
Ms 113B-191